Numerical analysis of the noisy Kuramoto-Sivashinsky equation in 2+1 dimensions

Jason T. Drotar, Y.-P. Zhao, T.-M. Lu, and G.-C. Wang
Department of Physics, Applied Physics, and Astronomy, Rensselaer Polytechnic Institute, Troy, New York 12180-3590
(Received 22 December 1997; revised manuscript received 30 September 1998)

The nondeterministic Kuramoto-Sivashinsky (KS) equation is solved numerically in $2+1$ dimensions. The simulations reveal the presence of early and late scaling regimes. The initial-time values for the growth exponent β, the roughness exponent α, and the dynamic exponent z are found to be 0.22–0.25, 0.75–0.80, and 3.0–4.0, respectively. For long times, the scaling exponents are notably less than the exponents of the Kardar-Parisi-Zhang equation. Other properties, such as skewness and kurtosis of the height distributions, are examined. We also compare the numerical analysis with recent experimental results on ion sputtering of surfaces that can be described by the KS equation. [S1063-651X(99)04601-2]

PACS number(s): 05.40.+j, 05.45.Pg

I. INTRODUCTION

The nondeterministic version of the Kuramoto-Sivashinsky (KS) equation can be used to describe the evolution of a surface ion-sputtered at normal incidence [1]. Furthermore, for dimensions other than $1+1$, many open questions remain, such as whether or not the KS equation exhibits the same scaling behavior as the Kardar-Parisi-Zhang (KPZ) equation [1]. This question, which has already been addressed for the deterministic case in $1+1$ dimensions [2], refers to the long-time (asymptotic) behavior of the KS equation. The KS equation is given by

$$\frac{\partial h}{\partial t} = \nu \nabla^2 h - \kappa \nabla^4 h + \frac{\lambda}{2} |\nabla h|^2 + \eta, \tag{1}$$

where h is the height of the interface (it is assumed that there are no overhangs). The noise term, η, satisfies

$$\langle \eta(\vec{r},t) \rangle = 0 \tag{2}$$

and

$$\langle \eta(\vec{r},t)\, \eta(\vec{r}',t') \rangle = 2D\, \delta(\vec{r}-\vec{r}')\, \delta(t-t'). \tag{3}$$

The parameter ν is generally negative for the KS equation in contrast to the KPZ equation in which the Laplacian term has a positive coefficient and corresponds to a surface tension. In the KS equation, the combination of the $\nabla^2 h$ and $|\nabla h|^2$ terms models the effect of particles being knocked out of the interface by the bombarding ions. For other than normal incidence, however, separate coefficients are needed in front of each term contained within $\nabla^2 h$ and $|\nabla h|^2$ (note that, without separate coefficients, we have rotational symmetry as we must for normal incidence). These terms can be derived from a simple model of ion bombardment in which the particles are assumed to penetrate a fixed distance into the interface and then spread their energy out with an asymmetric, three-dimensional Gaussian distribution [3,4]. The $-\nabla^4 h$ term models the effect of surface diffusion [5]. The noise term is present due to the randomness in the arrival of bombarding ions at the interface [4]. The $2D$ in Eq. (3) refers to the variance of the noise term and is proportional to the rate of bombardment [4].

The KS equation is believed to encompass many of the features that are actually realized in ion-sputtering experiments, such as ripple formation and KPZ-type scaling [6]. However, many ion-sputtering experiments show exponents that are not consistent with the KPZ exponents [7,8]. This is rather puzzling if we accept the KS equation as the equation describing ion sputtering. However, for different experimental conditions, the parameters in the KS equation will be different. This can lead to differences in the length and time scales over which scaling behavior is observed. In particular, for low-energy experiments, it is possible for the crossover times to become large enough to prevent the asymptotic behavior from being observed.

The belief that the KS equation scales, asymptotically, like the KPZ equation is based on analytical arguments [9] and on direct numerical verification in $1+1$ dimensions [2,6], but, so far, direct numerical verification has not been attempted in $2+1$ dimensions. The $(2+1)$-dimensional case is, physically, the most important case. In addition, it has been proposed that the KS equation cannot exhibit power-law scaling in $2+1$ dimensions [10]. Cuerno and Lauritsen have applied a renormalization-group analysis to the KS equation but were not able to obtain the values for the asymptotic exponents in $2+1$ dimensions [1]. The $(1+1)$-dimensional simulations of Sneppen *et al.* [2], for the deterministic case, and Cuerno *et al.* [6], for the nondeterministic case, reveal that crossover to KPZ behavior only occurs after the occurrence of early and intermediate scaling regimes, making it necessary to integrate the KS equation over extraordinarily long times. It is desirable to see the crossover to asymptotic KPZ behavior in $2+1$ dimensions.

The purpose of this study is to examine, in detail, the behavior of the KS equation. First, the early-time behavior is carefully examined. Then, guided by the qualitative aspects of the $(1+1)$-dimensional case, we extend the simulations to longer times and larger system sizes. The results show, not surprisingly, a crossover from the early-time behavior to another scaling regime. The exponents are close, but not equal, to the KPZ exponents.

II. METHOD OF SOLUTION

It is useful to perform a stability analysis by a Fourier transform of the linear terms of the KS equation. Denoting

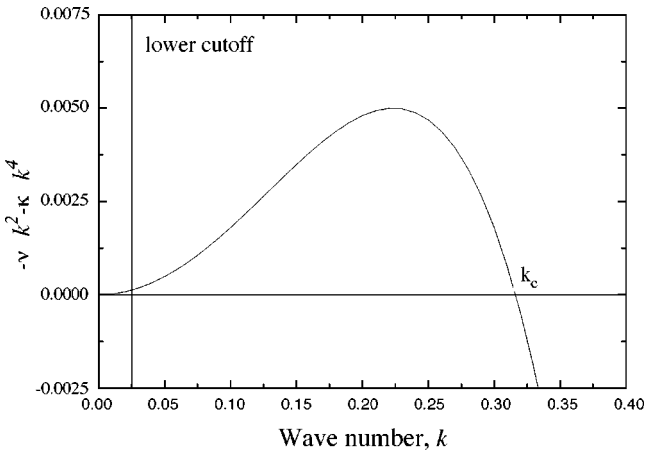

FIG. 1. Growth spectrum for the linear part of the KS equation with $\nu=-0.2$ and $\kappa=2.0$ with the lower cutoff for a 256×256 system shown.

the spatial Fourier transform of h by $F(h)$, we have

$$\frac{\partial F(h)}{\partial t}=-k^2\nu F(h)-k^4\kappa F(h), \tag{4}$$

where k is the wave number. This implies (considering only the linear terms) that periodic solutions with wave number k grow like $F(h)=e^{-(\nu k^2+\kappa k^4)t}$. Hence, if ν is negative, there will be a range of low frequencies that will grow exponentially. Figure 1 shows the corresponding stable and unstable regions. The critical wave number is given by $k_c=\sqrt{|\nu/\kappa|}$. Of course, the nonlinear part of the equation will also be a factor in the time evolution of the surface. According to Rost and Krug, the nonlinear term will couple modes with different wave numbers, thus stabilizing the equation [11].

The method used to solve the KS equation is a simple numerical integration. The first step is to write the equation as

$$\frac{\Delta h}{\Delta t}=\nu\nabla^2 h-\kappa\nabla^4 h+\frac{\lambda}{2}|\nabla h|^2+\left(\frac{24D}{\Delta t\Delta r^2}\right)^{1/2}R(\vec{r},t), \tag{5}$$

where $R(\vec{r},t)$ is an uncorrelated uniform noise distributed between -1 and $+1$. It is useful to rescale the KS equation using

$$h'=h/h_0,\quad \vec{r}\,'=\vec{r}/r_0,\quad t'=t/t_0. \tag{6}$$

If we let

$$h_0=\nu/\lambda,\quad r_0^2=\nu t_0,\quad t_0=\kappa/\nu^2, \tag{7}$$

we can eliminate all of the parameters from the equation except for the coupling constant

$$g=D\lambda^2/\nu^3. \tag{8}$$

This is the same coupling constant that is left over after rescaling the KPZ equation [12]. The random number generator used produces a uniform distribution and has an infinite period [13]. The solution of Eq. (5) is simply the solution to an initial value problem in which the surface is initially flat.

Because of the nonlinear term, the KS equation is stable, but extra care had to be taken to ensure numerical stability. The early-time simulations used the values $D=1$, $\Delta x=1$, and $\Delta t=0.005$, while the long-time simulations used $D=1$, $\Delta x=2$, and $\Delta t=0.05$. These were found to provide sufficient numerical stability for the parameter values used. Programming was done in C++.

From the numerical integration data, it was possible to determine the time-dependent height-height correlation function,

$$H(\vec{r},t)=\langle[h(\vec{r}+\vec{r}\,',t)-h(\vec{r}\,',t)]^2\rangle. \tag{9}$$

Here, h is the interface height and the averaging is done over the $\vec{r}\,'$ variable. If we assume that dynamic scaling still holds, the height-height correlation function will take the form [14]

$$H(\vec{r},t)=2[w(t)]^2 f\left(\frac{r}{\xi(t)}\right), \tag{10}$$

with $f(x)\propto x^{2\alpha}$ for $x\ll1$ and $f(x)=1$ for $x\gg1$. Here $w(t)$ is the interface width defined by $w(t)^2=\langle[h(\vec{r},t)-\overline{h}(\vec{r},t)]^2\rangle$, $\xi(t)$ is the lateral correlation length, and α is called the roughness exponent. In the scaling regime, both $w(t)$ and $\xi(t)$ evolve in time as power laws,

$$w\propto t^{\beta} \tag{11}$$

and

$$\xi\propto t^{1/z}. \tag{12}$$

Here β and z are the growth and dynamic exponents, respectively. In the dynamic scaling hypothesis, we have

$$z=\alpha/\beta. \tag{13}$$

For early times, each of the exponents were obtained by fitting the function [15]

$$H(r)=2w^2\left\{1-\exp\left[-\left(\frac{r}{\xi}\right)^{2\alpha}\right]\right\} \tag{14}$$

to the equal-time height-height correlation function. This function was fitted in log-log scale using an algorithm that minimized the least-square difference. Since the long-time height-height correlation functions do not have the form given in Eq. (14), these exponents had to be determined in a different way. For α, this is done by fitting a line to the $r\ll\xi$ part of the log-log plot of $H(r)$. The slope of this line is 2α. The growth exponent is found by fitting a line to the log-log plot of w. The slope of this line is β.

III. RESULTS

In each of the simulations, the parameter ν was fixed at $\nu=-0.2$, while the parameters λ and κ were varied. By varying λ, the coupling constant g could be varied. Varying κ made it possible to vary the extent of the instability in the linear terms. Of course, κ only affects the scaling in the presence of an upper or lower cutoff in k caused by a finite lattice spacing or finite system size, respectively. For the early-time simulations, a 256×256 lattice was used in each

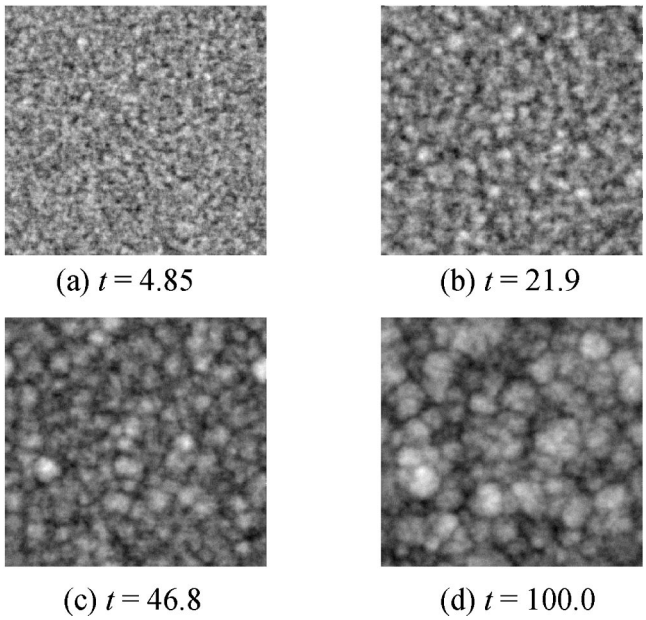

FIG. 2. Two-dimensional images for various growth times with the gray scale indicating the height h (dark indicates low h). Images are 256×256 with $\nu=-0.2$, $\kappa=2.0$, and $\lambda=1.0$. (a) $t=4.85$. (b) $t=21.9$. (c) $t=46.8$. (d) $t=100.0$.

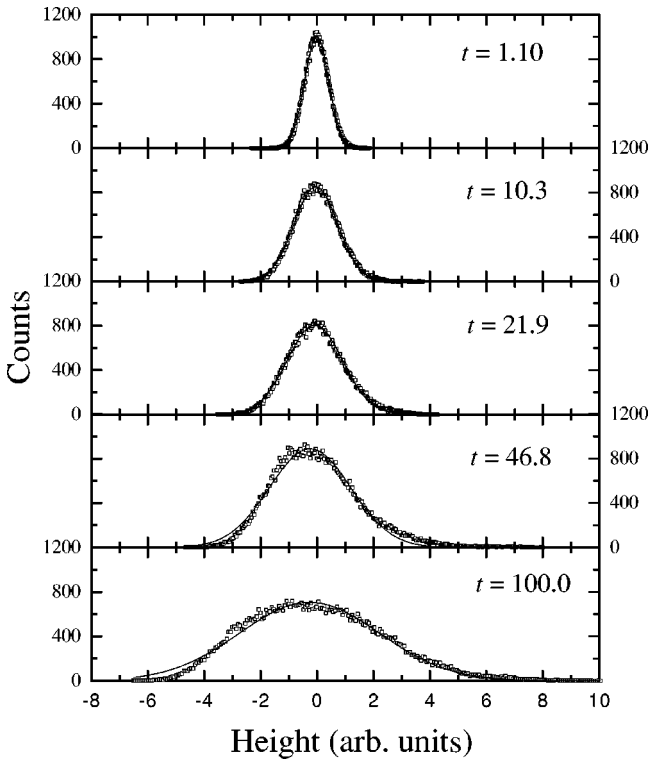

FIG. 3. Height distributions for various growth times with $\nu=-0.2$, $\kappa=2.0$, and $\lambda=1.0$.

simulation with $\Delta x=1$, and D was set equal to 1. The growth rates for low-frequency modes (due to the linear terms) are shown in Fig. 1 with $\nu=-0.2$ and $\kappa=2.0$. The lower cutoff for a system size of 256×256 is also shown. The upper cutoff due to $\Delta x=1$ is equal to 2π and is not shown. Clearly, the upper and lower cutoffs encompass most of the unstable portion of the growth spectrum.

Figure 2 shows the snapshots of surface morphology for $\nu=-0.2$, $\kappa=2.0$, and $\lambda=1.0$, at $t=4.85$, 21.9, 46.8, and 100, respectively. There are no obvious ''mounds'' formed on the surfaces. With the increase of the growth time, the lateral length of the surface features becomes bigger and bigger. Figure 3 shows the corresponding height distributions for these surfaces. Due to the presence of the noise term, the distribution of heights was expected to be close to a Gaussian distribution. The solid lines in Fig. 3 are the Gaussian best-fit curves. For early times, the distributions appear to be close to a Gaussian distribution, but at later times are skewed. This is not too surprising, because the $h\rightarrow-h$ symmetry is broken by the nonlinear $|\nabla h|^2$ term. The deviation from a Gaussian distribution can be characterized by skewness m_3 and kurtosis m_4, defined as

$$m_3=\frac{\langle[h(\vec{r})-\overline{h}(\vec{r})]^3\rangle}{w^3}, \tag{15}$$

$$m_4=\frac{\langle[h(\vec{r})-\overline{h}(\vec{r})]^4\rangle}{w^4}. \tag{16}$$

Skewness is a measure of the symmetry of a profile about the reference surface level. The sign of the skewness will tell whether the farther points are proportionately above (positive skewness) or below (negative skewness) the average surface level. Kurtosis is a measure of the sharpness of the height distribution function. If most of the surface features are concentrated near the mean surface level, the kurtosis will be less than if the height distribution contained a larger portion of the surface features lying farther from the mean surface level. In addition, kurtosis describes the randomness of the surface relative to that of a perfectly random surface (Gaussian distribution) that has a kurtosis of 3.0. Figure 4 plots the interface width w, the skewness m_3, and the kurtosis m_4 as functions of growth time for $\nu=-0.2$, $\kappa=2.0$, and $\lambda=1.0$. The log-log plot of the interface width w is a straight line for $t<10$ with an initial growth exponent $\beta\cong0.22-0.25$. This is close to the β value of the KPZ model [12]. After $t\cong30$, there is a dramatic change of β, from 0.24 to about 0.7, as shown in Fig. 4. Initially, the skewness is close to zero, and the kurtosis is close to 3. However, with the increase of the growth time, both the skewness and the kurtosis increase until a maximum is reached. The dramatic changes in both skewness and kurtosis occur slightly earlier than that for the interface width. This shows that the nonlinear term took action before the system became unstable.

To determine the roughness exponent and dynamic exponent, it was necessary to compute the height-height correlation function. This was done at 20 different times for each simulation and the results for $\nu=-0.2$, $\kappa=2.0$, and $\lambda=1.0$ are shown in Fig. 5. In the log-log plot, the time-dependent height-height correlation functions $H(r)$ at different times do not overlap for $r\ll\xi$, which demonstrates that the KS equation describes a growth process which is nonstationary for early times [16]. At this point, the roughness exponent α determined through Eq. (14) is near 0.75–0.85, which is quite different from the value of 0.38 that one obtains for the KPZ equation in $2+1$ dimensions [17].

It is very interesting to study the time-dependent behavior of the exponents. In Fig. 6, an average over 15 runs for both

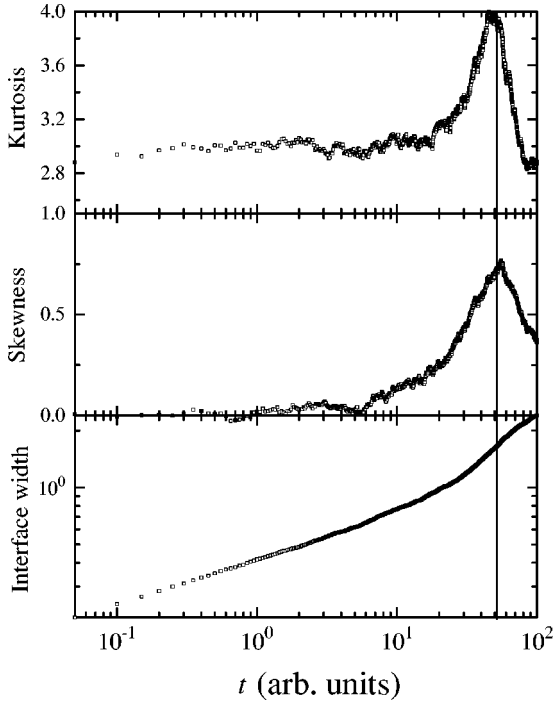

FIG. 4. Interface width, skewness, and kurtosis vs growth time for $\nu=-0.2$, $\kappa=2.0$, and $\lambda=1.0$.

α and β as a function of growth time t is shown. These were obtained by running 15 different simulations with different random number seeds. The error bars represent the standard deviation of the results. The results for z are shown in Fig. 7. The roughness exponent α remains almost the same throughout the growth, while the growth exponent β behaves differently. Initially β remains almost a constant, then at a certain time β starts increasing until a maximum is reached. Then β decreases. In their $(1+1)$-dimensional simulations, Sneppen *et al.* demonstrated that β can reach a maximum, after which β will decrease to a constant for longer growth time [2]. The same behavior can also be expected in $2+1$ dimensions.

We also investigated the effect of the growth coefficients λ and κ in the KS equation. Figures 8(a) and 8(b) plot the

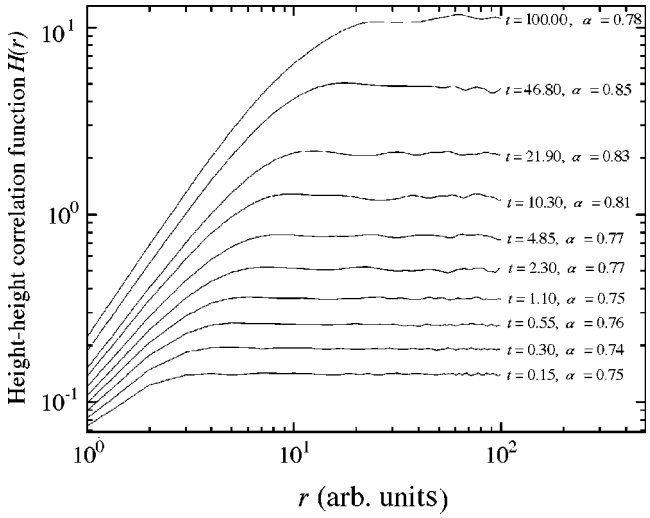

FIG. 5. Height-height correlation functions for various growth times for $\nu=-0.2$, $\kappa=2.0$, and $\lambda=1.0$.

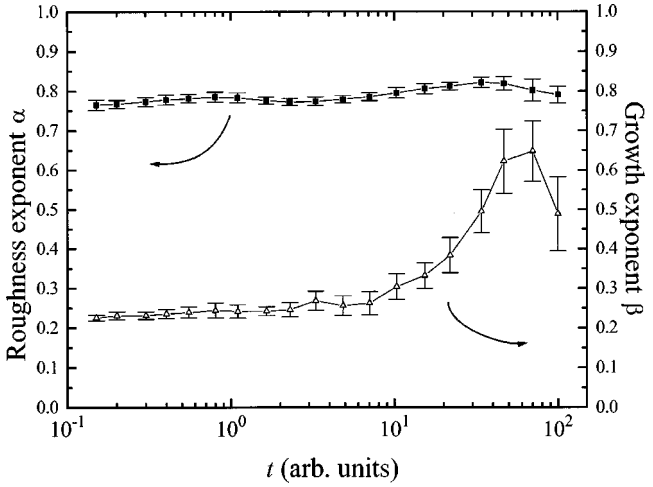

FIG. 6. Roughness exponent α and growth exponent β vs growth time with error bars for $\nu=-0.2$, $\kappa=2.0$, and $\lambda=1.0$ averaged over 15 runs.

growth exponent β and roughness exponent α as a function of growth time for various λ values. In fact, the change of the λ value affects the coupling constant g as shown in Eq. (8). The larger the λ value, the stronger the coupling. Clearly for each different λ, β has a similar behavior as described above. However, the onset of the increase in β occurs earlier for a stronger coupling. The change of λ also affects the behavior of α as shown in Fig. 8(b). Initially, α is the same for different λ. But at later times, α begins to decrease earlier as λ increases. The analytical result for $\lambda\rightarrow 0$ is shown in Fig. 8 as a dashed curve. This was obtained by computing the height-height correlation functions analytically for different times and fitting them the same way that the simulation data were fitted. The decrease in α in the analytical result for early times is due to the deviation in the shape of the early-time height-height correlation functions from the shape of the fitting function. As the coupling constant gets bigger, the effect of the nonlinear $|\nabla h|^2$ term becomes more important. This term has two impacts on the surface morphology, i.e., to make the spatial frequency higher and lower. For the initial

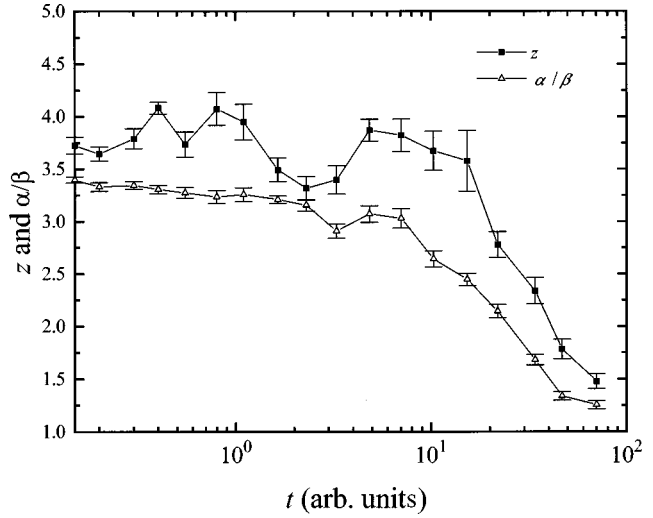

FIG. 7. Dynamic exponent z and α/β vs growth time with error bars for $\nu=-0.2$, $\kappa=2.0$, and $\lambda=1.0$ averaged over 15 runs.

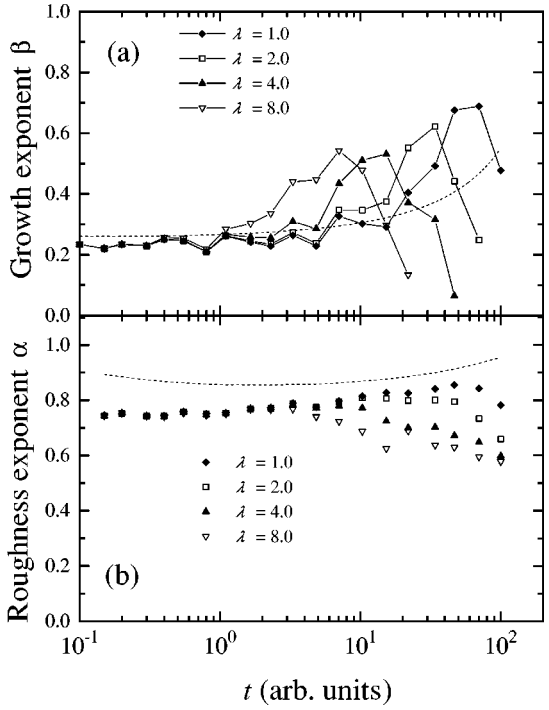

FIG. 8. (a) Growth exponent β vs growth time and (b) roughness exponent α vs growth time with $\nu=-0.2$, $\kappa=2.0$, and various λ. The dashed lines represent the analytical result for $\lambda=0$.

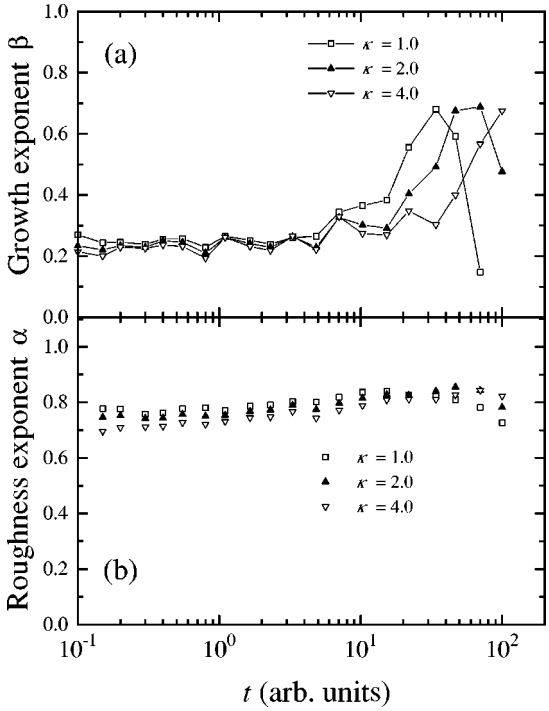

FIG. 9. (a) Growth exponent β vs growth time and (b) roughness exponent α vs growth time with $\nu=-0.2$, $\lambda=1.0$, and various κ.

stage, as the noise is a white noise, the nonlinear term will render the spatial frequency equally to the lower and higher end. However, the linear term will amplify low-frequency parts and eliminate high-frequency parts. Therefore, initially, the nonlinear term helps the low-frequency accumulation. Thus, α will increase slightly. Also β will increase. However, as the amplitude of the low-frequency components passes a certain value, the nonlinear term will start to eliminate the low-frequency part. That will reduce both the α and β values. Increasing the λ value will increase the rate of the coupling, thereby making the onset earlier.

A change of κ will also change the behavior of α and β as shown in Fig. 9. This change is different from that caused by varying λ. The initial β and α values are slightly different for different κ values. For later times, changing κ amounts to changing the location of the peak in β and not the height of it. This is consistent with the rescaling result $t_0=\kappa/\nu^2$. This is also understandable in terms of the stability of the equation. A higher value of κ will make the linear terms more stable for a given k, thus delaying the increase in β. The same behavior also occurs for α although it is much less obvious since the graph of α is relatively flat compared to that of β.

We also investigated the long-time behavior of the KS equation. The main difficulties in obtaining the long-time behavior of the KS equation were the need to increase the length of time over which the equation was integrated and the need to increase the system size enough to delay the onset of saturation. To delay saturation, we used a 512 $\times$512 lattice and set $\Delta x=2$. Figure 10 shows the interface widths and growth exponents for different values of λ. The growth exponent was close to 0.20 in each case. The height-height correlation functions for different times with $\lambda=2.0$ are shown in Fig. 11. There are two interesting features of this graph. First, the growth becomes stationary for later times. Second, for later times, the height-height correlation functions exhibit a bifractal structure with two different roughness exponents. For $\lambda=2.0$, the upper part has a roughness exponent of 0.27 and the lower part has a roughness exponent of 0.71. For $\lambda=1.0$, we obtained 0.28 and 0.76, while $\lambda=4.0$ yielded 0.25 and 0.65. The values for the growth exponent were found to be 0.21, 0.18, and 0.16 for $\lambda=1.0$, 2.0, and 4.0, respectively. For $\lambda=4.0$, a 1024

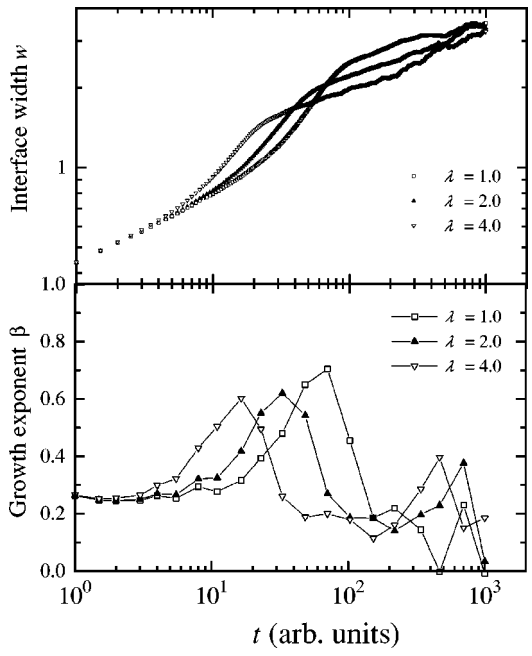

FIG. 10. Long-time values of interface width w and growth exponent β for $\nu=-0.2$, $\kappa=2.0$, and $\lambda=1.0$, 2.0, and 4.0.

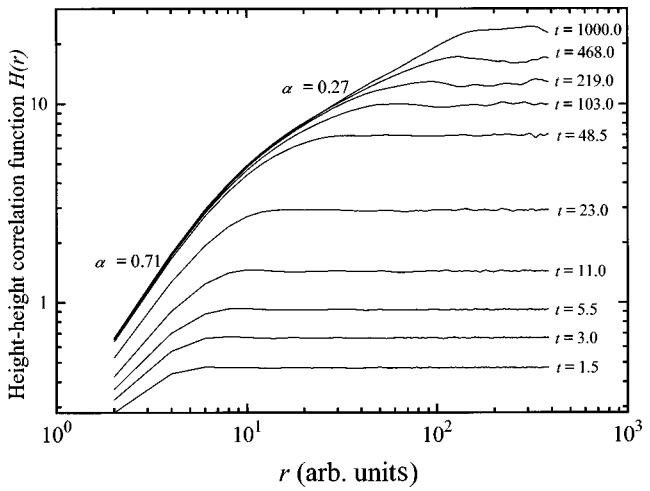

FIG. 11. Long-time height-height correlation functions for various growth times for $\nu=-0.2$, $\kappa=2.0$, and $\lambda=2.0$.

$\times 1024$ simulation was also run, and the interface width is shown in Fig. 12. Up to $t=2000$, there is still no sign of a crossover to another scaling regime.

IV. DISCUSSION

From a theoretical standpoint, the interesting aspects of the KS equation are its long-time scaling properties. The $(1+1)$-dimensional numerical results of Sneppen *et al.*, for the deterministic case, show the presence of early and intermediate scaling regimes, after which the growth exponent behaves like the $(1+1)$-dimensional KPZ exponent [2]. Our simulations clearly indicate the presence of an early-time scaling regime. If one looks just at the growth exponent, the early-time behavior is consistent with Mullins diffusion, but the roughness exponent is not consistent with just the $-\nabla^4 h$ term. Furthermore, these exponents cannot be explained by just the linear terms in the equation. Clearly, the interplay of the linear terms with the nonlinear term is responsible for the observed exponents, and it is only for very long times that one term in the equation dominates. What is not entirely clear is the nature of the late-time scaling regime. The growth and roughness exponents in this regime are notably less than the KPZ exponents. This could mean one of three things. First, it could mean that the asymptotic properties of the KS equation are not exactly those of the KPZ equation. Second, it could mean that our simulations have not yet reached the asymptotic regime. This second possibility is also supported by the presence of early, intermediate, and asymptotic regimes in the $(1+1)$-dimensional deterministic case. The third possibility is that our results might not correspond to the strong-coupling limit of the KPZ equation. Our own numerical integration of the KPZ equation shows a roughness exponent of 0.29 for $g=23$, which is very close to the long-time values we observe for the KS equation. However, Amar and Family find a roughness exponent of 0.39 for $g=50$ and 0.37 for $g=20$ [18]. This indicates that α might get smaller as the weak-coupling ($g=0$) limit is approached. Of course, the behavior should cross over to strong-coupling behavior for larger system sizes and longer times [18]. Hence, our late scaling regime might correspond to early-time KPZ behavior.

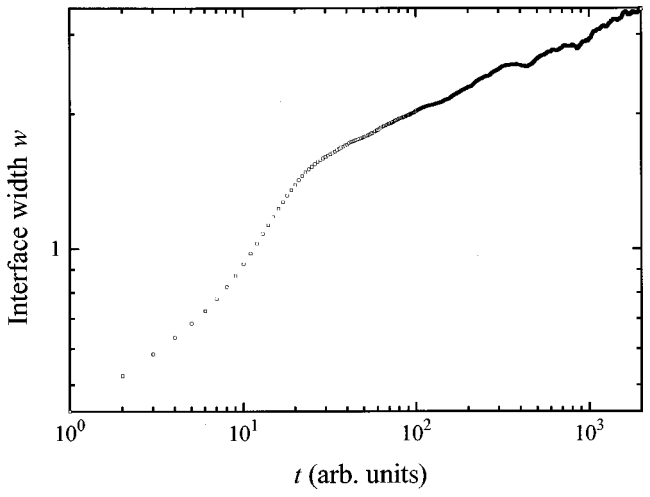

FIG. 12. Interface width for 1024×1024 long-time simulation with $\nu=-0.2$, $\kappa=2.0$, and $\lambda=4.0$.

It is also instructive to compare our results with other numerical results for the deterministic KS equation. Procaccia *et al.* have looked at the deterministic KS equation using direct integration [10]. They conclude that the long-wavelength properties of the deterministic KS equation in $2+1$ dimensions are not the same as those of the KPZ equation. In fact, they claim to show that $\alpha=0$. Our simulation results appear to contradict this result for the noisy KS, but Procaccia *et al.* do not speculate on whether their results should apply to the nondeterministic case. Furthermore, it is unlikely that even the deterministic $(2+1)$-dimensional KS equation exhibits only Edwards-Wilkinson behavior. Procaccia *et al.* find α by looking at the dependence of the saturation interface width versus system size. The log-log plot of w versus L is shown for L ranging between 32 and 512. How-

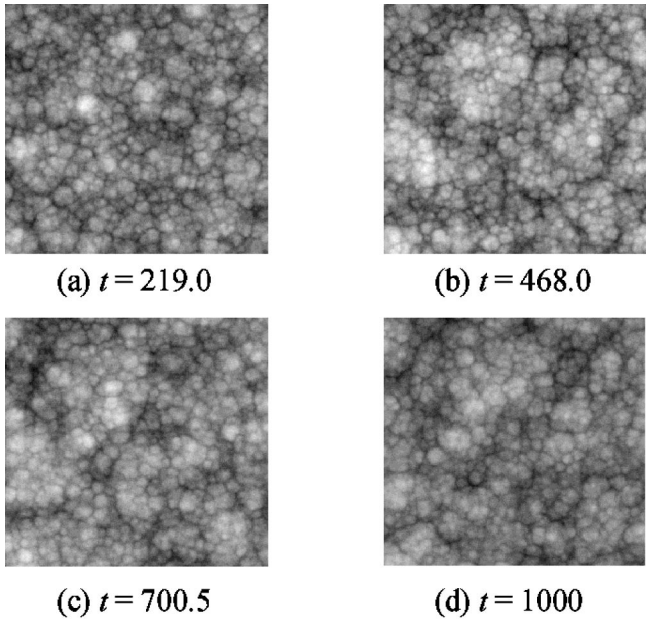

FIG. 13. Long-time two-dimensional images for various times. Images are 512×512 with $\Delta x=2.0$, $\nu=-2.0$, $\kappa=2.0$, and $\lambda=1.0$. Only a 256×256 portion is shown. (a) $t=219.0$. (b) $t=468.0$. (c) $t=700.5$. (d) $t=1000$.

TABLE I. The measured scaling exponents for several different ion-sputtering experiments are shown.

System	Method	Energy (eV)	α	β	Reference
Fe	STM	5000	0.53 ± 0.02		[19]
Si(111)	STM	500	0.7 ± 0.1	0.25 ± 0.05	[7]
Si(111)	HRLEED	500	1.15 ± 0.08		[20]
Ge(001)	X-ray diffraction	1000		0.1 ± 0.01, 0.4 ± 0.05	[21]
Ge(001)	STM	240	0.70 ± 0.03[a]		[8]
Graphite	STM	5000	0.2–0.4		[22]
GaAs(110)	STM	300–500		0.26, 0.31	[23]
GaAs(110)	STM	2000	0.38 ± 0.03		[24]
SiO_2	Energy-dispersive x-ray reflectivity	1000		1.0	[25]
SiO_2	Energy-dispersive x-ray reflectivity	150 300 1000		0.5	[26]

[a]This value was estimated from Fig. 3(b) of [8]. Also, the growth for this system is not self-affine [8].

ever, for system sizes as small as 32×32, saturation will occur very early, and the asymptotic behavior will not be observed; even with a 512×512 lattice it is difficult (if not impossible) to see the asymptotic behavior. Rost and Krug have done $(1+1)$-dimensional simulations of a particle model based on the KS equation [11]. Their model takes into account the cellular structure that evolves in systems described by the KS equation and gives exponents that coincide with the KPZ exponents [11]. While our results cannot be expected to agree with the $(1+1)$-dimensional case, we do see a cellular structure develop in the long-time surface morphology, as shown in Fig. 13. This cellular structure is also observed by Jayaprakash, Hayot, and Pandit in their $(2+1)$-dimensional simulations [9].

Cuerno *et al.* have done $(1+1)$-dimensional numerical integrations of the noisy KS equation [6]. Initially, they obtain a growth exponent consistent with Mullins diffusion, but, at later times, the growth exponent increases and then decreases to the Edwards-Wilkinson value. KPZ behavior is obtained for only a short amount of time before saturation occurs. This behavior is almost identical to the behavior obtained by Sneppen *et al.* for the deterministic case [2]. In our simulations, we obtain a region in which the growth exponent is consistent with Mullins diffusion, followed by a region in which β increases suddenly and then decreases; however, the region following this increase does not appear to be consistent with Edwards-Wilkinson growth ($\beta=0$).

The results of our simulations reveal exponents that, for early times, are quite different from those of the KPZ equation. The results of various ion-sputtering experiments are shown in Table I. For comparison, we list in Table II the theoretical results of the exponents predicted by different

TABLE II. The predicted scaling exponents for several different $(2+1)$-dimensional growth equations are shown.

$\partial h/\partial t=$	Name	α	β	z	Reference
η	Random deposition		0.5		[17]
$\nabla^2 h+\eta$	Edwards-Wilkinson	0	0	2	[17]
$\nabla^2 h+\lvert\nabla h\rvert^2+\eta$	KPZ	0.38	0.24	1.58	[17]
$-\nabla^4 h+\eta$	Mullins diffusion	1	$\frac{1}{4}$	4	[17]
$\nabla^2 h-\nabla^4 h+\eta$	General linear Equation	0–1[a]	0–0.25[a]	2–4[a]	[27]
$-\nabla^2 h-\nabla^4 h+\lvert\nabla h\rvert^2+\eta$	KS (early time)	0.75–0.80	0.22–0.25	3.0–4.0	This work
$-\nabla^2 h-\nabla^4 h+\lvert\nabla h\rvert^2+\eta$	KS (late time)	0.25–0.28	0.16–0.21		This work
$-\nabla^2 h-\nabla^4 h+\lvert\nabla h\rvert^2+\eta$	KS (early time) from RG approach	1		4	[1]

[a]These values are for finite system size and finite lattice spacing. For infinitely large system size and infinitely small lattice spacing, the exponents are equal to Mullin's diffusion values for early times and crossover to the Edwards-Wilkinson values for later times [27].

growth equations. The general trend is that the values of α for low-energy (less than 1 keV) sputtering tend to agree with the initial stage of our simulations, while the high-energy (greater than 1 keV) experiments have roughness exponents more consistent with the KPZ equation. In particular, an ion-sputtering experiment performed by Chan and Wang, using STM, shows agreement with the initial stage of our simulation results that is well within the experimental error [7]. The ion-sputtering result of Yang *et al.*, using a diffraction technique, shows $\alpha = 1.15 \pm 0.08$ [20]. This result is certainly not consistent with the KPZ equation, but neither is it consistent with our simulation results. A possible explanation for the high value of α is that Yang *et al.* assumed that the distribution of heights was a Gaussian. As Zhao *et al.* showed recently, if this criterion is not met, then the near out-of-phase diffraction analysis presented by Yang *et al.* would not be adequate for the extraction of α [28]. Also, one Ge(001) sputtering experiment shows a transition between two different scaling behaviors as a function of temperature or ion current [21], while another shows the development of ripples [29].

It is instructive to investigate the failure of our simulations in describing high-energy sputtering. The model used in constructing the KS equation relies on the assumption that the distribution of energy deposited by arriving ions is a Gaussian [4]. However, the assumption of a Gaussian distribution holds only for low ion energies and breaks down for high ion energies [30]. Furthermore, a higher energy will shorten the crossover time, allowing the KPZ behavior to be observed.

V. CONCLUSION

The simulations we have performed should be considered as a first step in explicitly demonstrating the scaling properties of the KS equation in $2+1$ dimensions. The long-time exponents are close to the KPZ exponents, but our results do not answer conclusively the question of whether the KS equation is in the same universality class as the KPZ equation. A firm answer to this question would require longer run times and larger system sizes in order to rule out the possibility that our observed long-time scaling regime is, in fact, an intermediate scaling regime.

ACKNOWLEDGMENTS

This work was supported by the NSF. J.T.D. thanks the Department of Education for financial support. We thank John Wedding for reading the manuscript and for useful discussions.

[1] Rodolfo Cuerno and Kent Bækgaard Lauritsen, Phys. Rev. E **52**, 4853 (1995).
[2] K. Sneppen, J. Krug, M. H. Jensen, C. Jayaprakash, and T. Bohr, Phys. Rev. A **46**, 7351 (1992).
[3] R. Mark Bradley and James M. E. Harper, J. Vac. Sci. Technol. A **6**, 2390 (1988).
[4] Rodolfo Cuerno and Albert-László Barabási, Phys. Rev. Lett. **74**, 4746 (1995).
[5] S. Das Sarma and P. Tamborenea, Phys. Rev. Lett. **66**, 325 (1991).
[6] Rodolfo Cuerno, Hernán A. Makse, Silvina Tomassone, Stephen T. Harrington, and H. Eugene Stanley, Phys. Rev. Lett. **75**, 4464 (1995).
[7] Anthony C.-T. Chan and G.-C. Wang, Surf. Sci. **414**, 17 (1998).
[8] S. Jay Chey, Joseph E. Van Nostrand, and David G. Cahill, in *Evolution of Epitaxial Structure and Morphology*, edited by A. Zangwill, D. Jesson, D. Chambliss, and R. Clarke, MRS Symposia Proceedings No. 399 (Materials Research Society, Pittsburgh, 1996), p. 221.
[9] C. Jayaprakash, F. Hayot, and Rahul Pandit, Phys. Rev. Lett. **71**, 12 (1993).
[10] Itamar Procaccia, Mogens H. Jensen, Victor S. L'vov, Kim Sneppen, and Reuven Zeitak, Phys. Rev. A **46**, 3220 (1992).
[11] Martin Rost and Joachim Krug, Physica D **88**, 1 (1995).
[12] Keye Moser, János Kertész, and Dietrich E. Wolf, Physica A **178**, 215 (1991).
[13] William H. Press, Brian P. Flannery, Saul A. Teukolsky, and William T. Vetterling, *Numerical Recipes in C—The Art of Scientific Computing* (Cambridge University Press, New York, 1988).
[14] F. Family and T. Vicsek, J. Phys. A **18**, L75 (1985); F. Family, Physica A **168**, 561 (1990).
[15] S. K. Sinha, E. B. Sirota, and S. Garott, Phys. Rev. B **38**, 2297 (1988).
[16] T.-M. Lu, H.-N. Yang, and G.-C. Wang, in *Fractal Aspects of Materials*, edited by Fereydoon Family, B. Sapoval, P. Meakin, and R. Wool, MRS Symposia Proceedings No. 367 (Materials Research Society, Pittsburgh, 1995), p. 283.
[17] A.-L. Barabási and H. E. Stanley, *Fractal Concepts in Surface Growth* (Cambridge University Press, Cambridge, 1995).
[18] Jacques G. Amar and Fereydoon Family, Phys. Rev. A **41**, 3399 (1990).
[19] J. Krim, I. Heyvaert, C. Van Haesendonck, and Y. Bruynseraede, Phys. Rev. Lett. **70**, 57 (1993).
[20] H.-N. Yang, G.-C. Wang, and T.-M. Lu, Phys. Rev. B **50**, 7635 (1994); H.-N. Yang, G.-C. Wang, and T.-M. Lu, *Diffraction from Rough Surfaces and Dynamic Growth Fronts* (World Scientific, Singapore, 1993).
[21] D.-M. Smilgies, P. J. Eng, E. Landemark, and M. Nielsen, Europhys. Lett. **38**, 447 (1997).
[22] Elliot A. Eklund, Eric J. Snyder, and R. Stanley Williams, Surf. Sci. **285**, 157 (1993).
[23] X.-S. Wang, R. J. Pechman, and J. H. Weaver, J. Vac. Sci. Technol. B **13**, 2031 (1995).
[24] X.-S. Wang, R. J. Pechman, and J. H. Weaver, Surf. Sci. **364**, L511 (1996).

[25] E. Chason and T. M. Mayer, Appl. Phys. Lett. **62**, 363 (1993).
[26] E. Chason, T. M. Mayer, and A. Payne, Appl. Phys. Lett. **60**, 2353 (1992).
[27] S. Majaniemi, T. Ala-Nissila, and J. Krug, Phys. Rev. B **53**, 8071 (1996).
[28] Y.-P. Zhao, G.-C. Wang, and T.-M. Lu, Phys. Rev. B **55**, 13 938 (1997).
[29] E. Chason, T. M. Mayer, B. K. Kellerman, D. T. McIlroy, and A. J. Howard, Phys. Rev. Lett. **72**, 3040 (1994).
[30] Peter Sigmund, Phys. Rev. **182**, 383 (1969).